Protein Expression and Purification 113 (2015) 72–78

Contents lists available at ScienceDirect

Protein Expression and Purification

journal homepage: www.elsevier.com/locate/yprep

Characterization of the LysR-type transcriptional regulator YcjZ-like from *Xylella fastidiosa* overexpressed in *Escherichia coli*

André S. Santiago [a], Clelton A. Santos [a], Juliano S. Mendes [a], Marcelo A.S. Toledo [a], Lilian L. Beloti [a], Alessandra A. Souza [b], Anete P. Souza [a,c,*]

[a] Centro de Biologia Molecular e Engenharia Genética (CBMEG), Universidade Estadual de Campinas, Campinas, SP, Brazil
[b] Centro APTA Citros Sylvio Moreira/IAC, Rodovia Anhanguera Km 158, Cordeirópolis, SP, Brazil
[c] Departamento de Biologia Vegetal, Instituto de Biologia (IB), Universidade Estadual de Campinas, Campinas, SP, Brazil

ARTICLE INFO

Article history:
Received 27 January 2015
and in revised form 4 May 2015
Available online 12 May 2015

Keywords:
Xylella fastidiosa
Biofilm
YcjZ
Transcriptional regulator

ABSTRACT

The *Xylella fastidiosa* 9a5c strain is a xylem-limited phytopathogen that is the causal agent of citrus variegated chlorosis (CVC). This bacterium is able to form a biofilm and occlude the xylem vessels of susceptible plants, which leads to significant agricultural and economic losses. Biofilms are associated with bacterial pathogenicity because they are very resistant to antibiotics and other metal-based chemicals that are used in agriculture. The *X. fastidiosa* YcjZ-like (XfYcjZ-like) protein belongs to the LysR-type transcriptional regulator (LTTR) family and is involved in various cellular functions that range from quorum sensing to bacterial survival. In the present study, we report the cloning, expression and purification of XfYcjZ-like, which was overexpressed in *Escherichia coli*. The secondary folding of the recombinant and purified protein was assessed by circular dichroism, which revealed that XfYcjZ-like contains a typical α/β fold. An initial hydrodynamic characterization showed that XfYcjZ-like is a globular tetramer in solution. In addition, using a polyclonal antibody against XfYcjZ-like, we assessed the expression profile of this protein during the different developmental phases of *X. fastidiosa* in *in vitro* cultivated biofilm cells and demonstrated that XfYcjZ-like is upregulated in planktonic cells in response to a copper shock treatment. Finally, the ability of XfYcjZ-like to interact with its own predicted promoter was confirmed *in vitro*, which is a typical feature of LysR. Taken together, our findings indicated that the XfYcjZ-like protein is involved in both the organization of the architecture and the maturation of the bacterial biofilm and that it is responsive to oxidative stress.

Introduction

Xylella fastidiosa is a gram-negative, xylem-limited bacterium whose full genome is available [1]. The *X. fastidiosa* 9a5c strain is the causal agent of citrus variegated chlorosis (CVC), which is also known as "*amarelinho*" in Brazil. This bacterium is able to form a biofilm structure inside the xylem vessels of susceptible plants, which results in hydric impairment, a decrease in nutrients and, ultimately, plant death during the later stages of disease. Therefore, this bacterium is associated with great economic losses in São Paulo, which is the highest producer of concentrated orange juice in Brazil [2]. To prevent the *X. fastidiosa* from spreading in the field, copper-based chemicals are used [3], which cause bacterial oxidative stress, among other effects [4–6]; however, living organisms have a large repertoire of responses to stress conditions, including modulation of the gene expression profile and increased production of transcriptional regulators, which allow them to protect themselves and to adapt and survive under these conditions [7].

LysR-type proteins are members of the largest family of transcription regulators (LTTRs)[1] in prokaryotes and are highly conserved in the bacteria kingdom [8,9]. The proteins in this family are involved in numerous cellular functions, including oxidative stress responses [10], cell wall shape [11], quorum sensing [12], efflux pumps, secretion, motility [13], nitrogen fixation [14], virulence [15], cell division [16], metabolism and environmental recog-

* Corresponding author at: Centro de Biologia Molecular e Engenharia Genética (CBMEG), Universidade Estadual de Campinas, CP 6010, 13083-875 Campinas, São Paulo, Brazil. Tel./fax: +55 19 3521 1089.
E-mail address: anete@unicamp.br (A.P. Souza).

[1] *Abbreviations used:* LTTR, LysR-type transcriptional regulators; XfYcjZ-like, YcjZ of *X. fastidiosa*; HTH, helix-turn-helix; SEC, size-exclusion chromatography; AUC, analytical ultracentrifugation; CD, circular dichroism; EMSA, electrophoresis mobility shift assay.

http://dx.doi.org/10.1016/j.pep.2015.05.003
1046-5928/

nition [17]. Initially, LTTRs were classified as repressors [18,19]; however, as previously reported, they can also act as activators, depending on the circumstances and the signaling molecules [20]. LTTRs share a high degree of conservation in the helix-turn-helix (HTH) domain at the N-terminus, which is directly involved in DNA binding, whereas the C-terminus, which possesses the regulatory domains (RD) 1 and 2 that are co-inducer binding sites [21–23], exhibits low amino acid conservation.

In the present study, we report the initial functional and hydrodynamic characterization of a LysR-type transcriptional regulator called YcjZ-like from *X. fastidiosa* strain 9a5c (XfYcjZ-like). Recombinant XfYcjZ-like was overexpressed in an *Escherichia coli* host and purified by two-step chromatography. An initial structural analysis confirmed the secondary and tertiary structures of the recombinant and purified protein. We used a polyclonal antibody against XfYcjZ-like to confirm the expression profile of this protein during the biofilm growth of *X. fastidiosa* and demonstrated that XfYcjZ-like was able to respond to a copper shock treatment because it was upregulated in planktonic cells. In addition, the interaction of XfYcjZ-like with its own predicted promoter was analyzed *in vitro*. Our results provide new information regarding the involvement of the XfYcjZ-like transcription regulator in bacterial pathogenicity.

Materials and methods

Bacterial strain, amplification, plasmid and cloning

The coding sequence of XfYcjZ-like (975 pb; NCBI Reference Sequence: WP_010894223.1) was amplified from *X. fastidiosa* 9a5c genomic DNA by PCR using specific primers designed with a *Nde*I restriction site in the forward primer (5′-GGCCATATGGCCAG ACGCAAC-3′) and an *Xho*I site in the reverse primer (5′-CACGCTCGAGTTGGCGATGG-3′). The PCR program used for *xfycjZ*-like amplification included a denaturation step at 94 °C for 120 s, followed by an annealing step at 56 °C for 45 s and a final step at 72 °C for 90 s. This cycle was repeated 30 times. After PCR amplification, the amplicon was inserted into the pET28a vector using standard molecular biology methods [24], which added a His_6-tag to the N-terminus. The recombinant vector that was generated was subjected to DNA sequencing to confirm that the cloned sequence did not contain any base substitutions.

Amino acid sequence alignment and protein structure prediction

The amino acid sequence alignment between XfYcjZ-like and the *E. coli* YcjZ protein (EcYcjZ; GenBank ID EOQ56594.1) was analyzed using the ClustalW2 server (http://www.ebi.ac.uk/Tools/msa/clustalw2/). Structural modeling prediction of XfYcjZ-like was performed using the I-TASSER server (http://zhanglab.ccmb.med.umich.edu/I-TASSER/) [25].

XfYcjZ-like expression and purification

Positive colonies, carrying the pET28:*xfycjZ*-like construct, were grown in a pre-inoculated 10 mL of Luria–Bertani (LB) broth containing 30 μg mL^{-1} kanamycin at 37 °C and 250 rpm for 12 h and were then transferred to 1 L of LB broth and grown at the same conditions until an OD_{600} of 0.9 was reached. The cultures were then induced with 5.6 mmol L^{-1} lactose for 12 h at 22 °C. The cells were collected by centrifugation at 8000 rpm, 8 °C.

To perform protein extraction, the cells were resuspended in 50 mmol mL^{-1} phosphate buffer, pH 7.8, 300 mmol mL^{-1} NaCl and 10 mmol mL^{-1} β-mercaptoethanol (buffer A) and sonicated using the Ultrasonic Homogenizer 4710 series instrument (Cole-Parmer instrument Co., Chicago, IL, USA) set at 70% duty cycle, with 1 min on and 5 min off on ice.

For recombinant protein purification, the cell lysate was clarified by centrifugation at 16,000×*g* for 45 min at 5 °C and loaded on a column with Ni-NTA agarose superflow (Qiagen; Hilden, Germany) and eluted with an imidazole gradient, from 0 until 500 mmol L^{-1} in buffer A. Subsequently, the purity was estimated by running the proteins on a 12% sodium dodecyl sulfate polyacrylamide gel electrophoresis (SDS–PAGE) gel, which was stained using Coomassie Brilliant Blue R-250 (USB, Cleveland, OH, USA).

Analytical size-exclusion chromatography (SEC)

Analytical size-exclusion chromatography (SEC) experiments were performed on an AKTA FPLC system using a Superdex 200 10/300 GL prepacked column (GE Healthcare – Pittsburgh, PA, USA) that was previously equilibrated with buffer A. Aliquots of 500 μL of protein (approximately 25 μmol L^{-1}) were loaded onto the column at a flow rate of 0.5 mL min^{-1}, and the elution profile was monitored by the absorbance at 280 nm. To estimate the Stokes radius (R_s) of the recombinant XfYcjZ-like protein, a mix of protein standards with known R_s, including carbonic anhydrase (Mw = 29 kDa, 23.9 Å), ovalbumin (Mw = 44 kDa, 30.5 Å), conalbumin (Mw = 75 kDa, 36.4 Å), aldolase (Mw = 158 kDa, 48.1 Å) and ferritin (Mw = 440 kDa, 61 Å) were used to calibrate the column. All of the protein standards (GE Healthcare) were prepared at a concentration of 3 mg mL^{-1} in buffer A. The void volume of the column was determined using blue dextran (GE Healthcare). The elution profiles obtained for the recombinant XfYcjZ-like and standard protein were converted to the partition coefficient Kav using the following formula:

$$\mathrm{Kav} = \frac{\mathrm{Ve} - V_0}{\mathrm{Vt} - V_0}$$

where Ve is the elution volume of the protein, V_0 is the void volume of the column and Vt is the total column volume (24 mL). The XfYcjZ-like R_s was calculated by the adjusted linear fitting of the R_s of the standard proteins plotted against the $-(\log \mathrm{Kav})^{1/2}$. The experimental R_s obtained from the SEC analysis was used to estimate the frictional ratio (f/f_0) as the ratio of the experimental R_s to the radius of a sphere of the same molecular mass.

Measurement of circular dichroism

Circular dichroism (CD) spectra of the purified His_6-tagged XfYcjZ-like protein were measured using a Jasco J-810 Spectropolarimeter dichrograph (Japan Spectroscopic, Tokyo, Japan). The far-UV CD spectra were generated at 25 °C from a 13.6 μmol L^{-1} solution in 10 mmol L^{-1} sodium phosphate buffer at pH 7.8. The assays were carried out using a quartz cuvette with a 2 mm path length. Ten measurements within the 260–190 nm range at a rate of 20 nm min^{-1} were recorded. The deconvolution of the CD spectrum was performed using the DICRHOWEB server (http://dichroweb.cryst.bbk.ac.uk/).

Analytical ultracentrifugation measurements

Sedimentation velocity experiments of the XfYcjZ-like protein were carried out at concentrations ranging from 0.2 to 0.7 mg mL^{-1} in buffer A using a Beckman Optima XL-A analytical ultracentrifuge. Data acquisition during analytical ultracentrifugation (AUC) was performed at 280 nm, 20 °C, and 35,000 rpm using an AN-50Ti rotor. The AUC data analyses were performed with SedFit software (Version 12.1). The experimental *s*-value was calculated for the standard sedimentation coefficient at a concentration of 0 mg mL^{-1} of protein ($s^0_{20,w}$) to prevent interferences

derived from the buffer density, viscosity and temperature [26] by using the linear fitting of the curve of the $s_{20,w}$-value as a function of the protein concentration. The buffer viscosity ($\eta = 1.0513 \times 10^{-2}$ poise), buffer density ($\rho = 1.0163$ g mL^{-1}) and partial-specific XfYcjZ-like volume (Vbar: XfYcjZ-like = 0.733194 mL g^{-1}) used for the analysis were estimated by the Sednterp server (http://sednterp.unh.edu/). The R_s, MMpred, $s^0_{20,w}$ and f/f_0 for XfYcjZ-like were obtained from the AUC data analyses by SedFit.

Electrophoretic mobility shift assay (EMSA)

The XfYcjZ-like promoter identified in the *X. fastidiosa* 9a5c genome (NCBI Reference Sequence: NC_002488.3) was cloned, and its recognition and interaction with the recombinant purified XfYcjZ-like protein were analyzed by EMSA. The cloned region comprised a 262 bp DNA fragment that was upstream of the open reading frame (ORF) that encodes XfYcjZ-like and was cloned with the following specific primers: 5′-TTCGAGGGCGAACGGGAGGC-3′ and 5′-TGCGTCTGGCCATGGCGC-3′, forward and reverse, respectively. For the EMSA, the DNA fragment was incubated with the XfYcjZ-like protein in its tetrameric form at the following DNA:protein molar ratios: 1:0, 1:1, 1:2, 1:4, 1:8, 1:16, 1:32, 1:64 and 1:100 using the promoter at 11.76 nmol mL^{-1} in 10 mmol L^{-1} phosphate buffer, 150 mmol L^{-1} NaCl. Then, the mix was resolved by agarose electrophoresis using a 1.5% agarose gel run at 40 V for 3 h. Subsequently, the gel was stained with ethidium bromide and analyzed using the Kodak Electrophoresis Documentation and Analysis System (EDAS).

Western blotting analysis

Polyclonal antibodies against XfYcjZ-like were produced by Rheabiotech (Campinas, SP, Brazil) and used in the XfYcjZ-like immunodetection assays. To conduct copper shock, the bacteria were treated with a sublethal concentration of 1 mM $CuSO_4$ for 24 h prior to the collection day, and the control cells were collected during the days mentioned below. The total protein (approximately 5 μg) from *X. fastidiosa* 9a5c after 3, 5, 10, 15, 20 and 30 days of development was extracted according to [27] and loaded on a 12% SDS–PAGE gel. After separation, the proteins were transferred in triplicate to a nitrocellulose membrane using a Trans-Blot SD Semi-Dry Transfer Cell (Bio-Rad). The membranes were blocked with casein for 12 h and washed 3 times for 10 min with Tris-buffered saline and 0.1% tween 20 (TTBS) (NaCl 0.137 mmol L^{-1}, KCl 0.025 mmol L^{-1}, Tris 0.025 mmol L^{-1}, pH 7.5). The membrane was incubated with the primary antibody (anti-XfYcjZ-like) in a 1–4000 dilution for 6 h, washed under the same conditions as described previously and then incubated with alkaline phosphatase-conjugated anti-rabbit IgG (Santa Cruz Biotechnology Inc.; USA) for 4 h, followed by another set of washes with TTBS and incubation with the revelation buffer (Tris 100 mmol L^{-1}, NaCl 100 mmol L^{-1}, $MgCl_2$ 5 mmol L^{-1}, pH 9.0) with nitro blue tetrazolium/5-bromo-4-chloro-3-indolyl phosphate (NBT/BCIP; Sigma, USA), following the manufacturer's instructions.

Results and discussion

Alignment of XfYcjZ-like with its E. coli homolog and structural prediction analysis

XfYcjZ-like (324 amino acid residues) in the *X. fastidiosa* 9a5c genome was annotated as a LTTR protein that is involved in bacterial pathogenicity [1]. The alignment of the XfYcjZ-like amino sequence with that of *E. coli* YcjZ (Fig. 1A) showed a high degree of identity (approximately 58%), hence the name XfYcjZ-like. The LTTRs are described as being well conserved among bacteria [21,28], and this protein family encompasses approximately 800 members that have been identified based on their amino acid sequence identity [9]. In the XfYcjZ-like N-terminal domain that contains the HTH motif involved in DNA-binding, the identity with the homologous EcYcjZ region is even greater, reaching 65%; however, notable differences are observed between the C-terminal domains. XfYcjZ-like contains 27 C-terminal amino acid residues that are not present in the homologous *E. coli* protein. Because the LTTR C-terminal domain is described as containing co-inducer binding sites [21–23], this observation suggests that different co-inducers than those that act in *E. coli* can modulate the activity of XfYcjZ-like.

To obtain information about the predicted structure of XfYcjZ-like, we used the I-TASSER server to generate a putative model of its protein structure (Fig. 1B). Although no YcjZ homolog structure is available in the Protein Data Bank (PDB; http://www.rcsb.org), the predicted model of XfYcjZ-like showed a TM-score of 0.884 for the structural alignment between the query structure (XfYcjZ-like) and the known structure of AphB, a LTTR family gene activator from *Vibrio cholerae* (PDB code 3SZP) [29]. The TM-score is a proposed scale for measuring the structural similarity between two structures [30]; thus, the TM-score value obtained in this study indicates that the predicted XfYcjZ-like model contains the correct topology. The predicted XfYcjZ-like model showed an N-terminal DNA-binding domain in a typical HTH fold that was composed of three α-helices (α1–α3) followed by two β-strands (β1 and β2), whereas the C-terminal domain showed a typical α/β fold (Fig. 1B). Therefore, although we show only a putative model for XfYcjZ-like, it presents features similar to those of another LTTR protein whose structure is available [21,29].

Recombinant XfYcjZ-like was overexpressed and obtained in a soluble form with a dominant α-helical structure

In this study, XfYcjZ-like was cloned, and the recombinant protein was overexpressed in *E. coli* and purified using chromatographic methods. After the affinity chromatography step, a band of approximately 38.5 kDa, which corresponds to the size of the amino acid sequence of XfYcjZ-like plus the N-terminal His_6-tag added by the pET28a vector, was observed on a 12% SDS–PAGE gel (Fig. 2A). The recombinant protein was mostly present in the soluble fraction and resulted in a yield of 4 mg of purified protein per liter of bacterial culture. The purified XfYcjZ-like fraction remained stable in solution and showed no protein degradation for several days. The secondary structure of the recombinant and purified XfYcjZ-like was evaluated by CD (Fig. 2B). The CD analysis of the recombinant protein revealed that XfYcjZ-like has a typical spectrum for a protein that is rich in α-helical structures and is approximately 36.7% α-helix structure, 15% β-sheet and 38% random coil. The CD spectrum deconvolution matched the modeling analysis and strengthens the structural prediction of XfYcjZ-like by I-TASSER (Fig. 1B), in which the N-terminal α-helix rich DNA-binding HTH motif was observed.

Hydrodynamic characterization of XfYcjZ-like

We employed analytical SEC and AUC to evaluate the characteristics of the recombinant, purified XfYcjZ-like protein in solution. Table 1 summarizes the results obtained from the hydrodynamic characterization of XfYcjZ-like. XfYcjZ-like was eluted as a unique peak during the analytical SEC experiments (Fig. 3A), with a retention profile corresponding to an apparent molecular mass (MM_{app}) of 159 ± 4 kDa and R_s of 44.4 ± 1 Å (Fig. 3B). By comparing the predicted hydrodynamic data from the amino acid sequence of

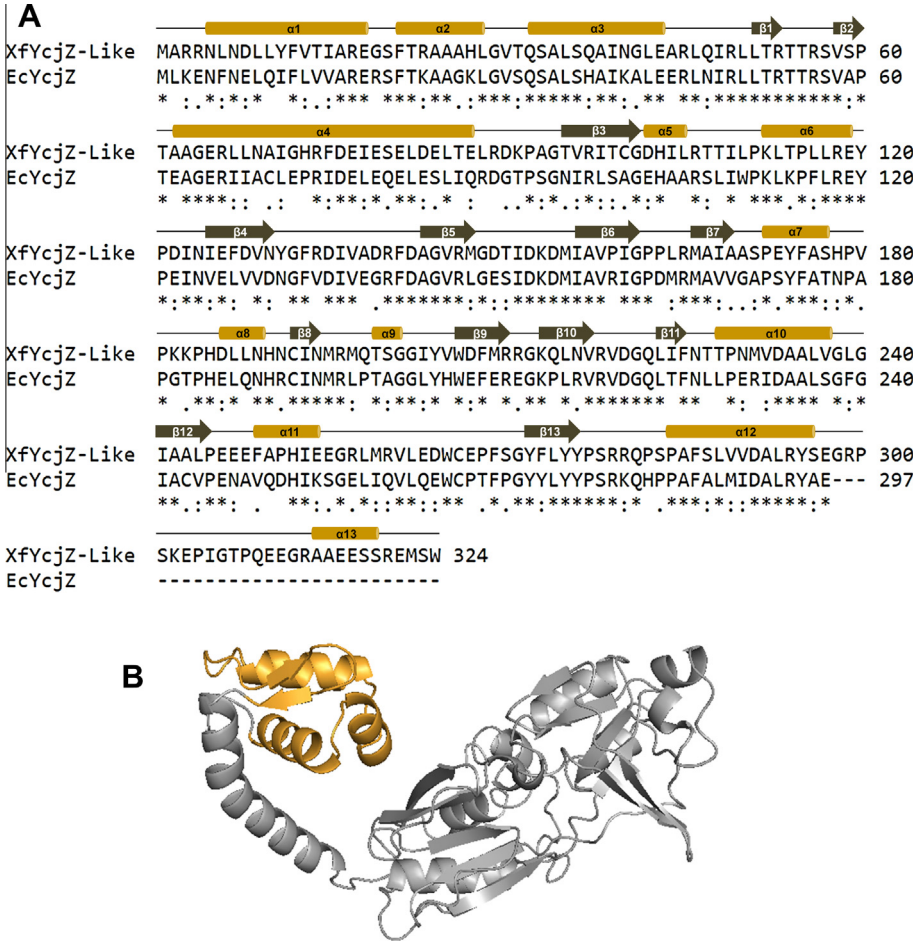

Fig. 1. XfYcjZ-like sequence alignment analysis and protein structure prediction. (A) The amino acid sequences of XfYcjZ-like (NCBI Reference Sequence: WP_010894223.1) and the *E. coli* YcjZ protein (EcYcjZ; GenBank ID EOQ56594.1), were aligned using the ClustalW2 server (http://www.ebi.ac.uk/Tools/msa/clustalw2/), which revealed high identity (58%). Conservation between identical amino acid residues is indicated by an asterisk, residues with strongly similar properties are shown by a double dot and weakly similar properties are represented by a single dot. (B) Structural modeling prediction of XfYcjZ-like. The N-terminal DNA-binding motif (residues 1–60) is highlighted in gold in the model with the best C-score. The modeling prediction was performed using the I-TASSER server (http://zhanglab.ccmb.med.umich.edu/I-TASSER/). (For interpretation of the references to color in this figure legend, the reader is referred to the web version of this article.)

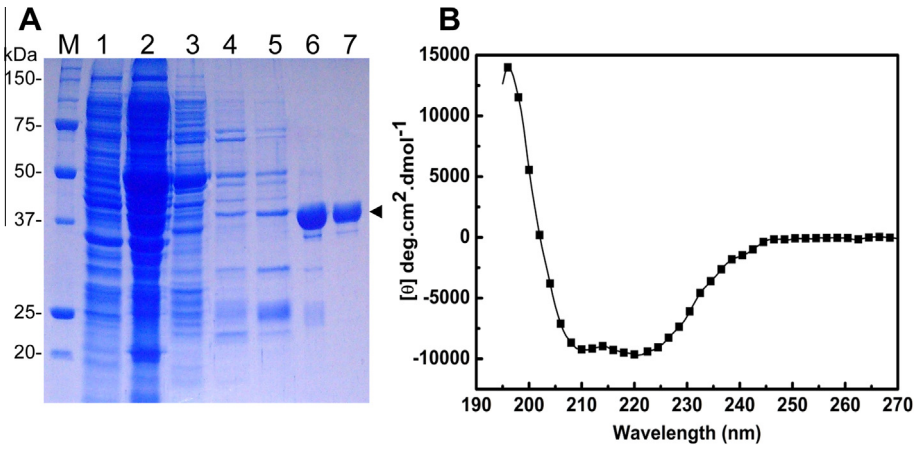

Fig. 2. XfYcjZ-like protein purification and secondary structural analysis. (A) SDS–PAGE 12% gel showing XfYcjZ-like protein purification. M: molecular mass markers; lane 1, cell lysate before protein induction; lane 2, cell lysate after protein induction; lanes 3–6, proteins eluted using an imidazole gradient (20, 50, 75 and 100 mmol L^{-1}, respectively); lane 7, protein after size exclusion chromatography. The recombinant purified XfYcjZ-like is indicated by a black left-pointing triangle. The protein purification-yielded proteins with a purity greater than 95%. (B) Circular dichroism spectra of XfYcjZ-like. The CD results suggested that XfYcjZ-like is rich in α-helical structures.

XfYcjZ-like with the experimental SEC data (Table 1 and Fig. 3A and B), the recombinant purified XfYcjZ-like is possibly a tetramer in solution and shows an f/f_0 value of 1.25. This result is expected for a protein with a globular shape. From the AUC data analysis, our findings indicate that XfYcjZ-like sediments as a single species with $s^0_{20,w}$ and an experimental molecular mass (MM_{exp})

Table 1
Hydrodynamic properties of recombinant purified XfYcjZ-like protein.

Technique	Property
Predicted hydrodynamic data[a]	Monomer = R_0 22.4 Å, MM_{pred} 38.5 kDa Dimer = R_0 28.2 Å, MM_{pred} 77.1 kDa Tetramer = R_0 35.5 Å, MM_{pred} 154.2 kDa
SEC	R_s 44.4 ± 1 Å MM_{app} 159 ± 4 kDa f/f_0[b] 1.25
AUC	$s^0_{20,w}$ (S) 6.65 ± 0.02 f/f_0[c] 1.36 ± 0.1 MM_{exp} 151 ± 2 kDa R_s 46 ± 2 Å

[a] Predicted from the amino acid sequence using the Sednterp server (http://sednterp.unh.edu/).
[b] From the ratio of R_s obtained from SEC analyses by R_0 of the tetramer predicted data.
[c] Obtained from SedFit analysis.

of 6.65 ± 0.02 S and 151 ± 2 kDa, respectively, which suggests that it behaves as a tetramer in solution (Fig. 3C and D; Table 1). The AUC sedimentation velocity data also indicated that XfYcjZ-like exhibited an f/f_0 of 1.36 ± 0.1 and R_s of 46 ± 2, suggesting that it has a globular shape. The AUC data corroborated the analytical SEC results and confirmed the tetrameric state of XfYcjZ-like in solution.

The oligomeric states of the LTTR proteins in solution have been described as dimers and tetramers, although octameric forms have also been observed [10,13,29,31]. The tetrameric state is reported as the most common oligomeric form of the LTTR proteins because this conformation correctly positions the HTH domain to facilitate protein:DNA interactions, although the tetramer must undergo a conformational change for DNA binding to occur [29].

Interaction with its promoter

The ability of recombinant XfYcjZ-like to interact with DNA was investigated by EMSA. We initially searched for the predicted promoter of the *xfycjZ*-like gene in the *X. fastidiosa* genome [1]. A 262 bp DNA sequence upstream of *xfycjZ*-like contains all of the regulatory regions required for a promoter (Fig. 4A) and was used for the protein:DNA binding experiments. The LTTRs recognize specific pseudopalindromic DNA sequences, e.g., ATC-N_9-GAT [32] and T-N_{11}-A [33], that permit protein:DNA interactions and subsequent gene regulation. The predicted *xfycjZ*-like promoter contains five T-N_{11}-A DNA sequences: −12 to −24; −37 to −49, −59 to −71, −87 to −99 and −102 to −114 (Fig. 4A).

Our results showed that the recombinant and purified XfYcjZ-like protein was able to interact *in vitro* with its cis-regulatory element at a molar ratio as low as 1:2 (DNA:protein) and showed a 96% interaction rate at a 1:16 ratio, which led to a shift in the mobility of the DNA fragment (Fig. 4B). We therefore concluded that recombinant XfYcjZ-like was produced in an active and folded state.

XfYcjZ-like immunoblotting during X. fastidiosa growth

Polyclonal antibodies against XfYcjZ-like were used to assess the protein expression profile during different phases of *X. fastidiosa* biofilm growth and in associated planktonic cells. XfYcjZ-like was differentially expressed during biofilm formation and planktonic growth of *X. fastidiosa*. XfYcjZ-like was strongly detected until 15 days of planktonic growth, whereas in the biofilm cells, higher levels of protein expression were detected at 5 and 20 days (Fig. 5A). The *X. fastidiosa* biofilm developmental process was described previously [27]. On the 5th day, microcolony formation

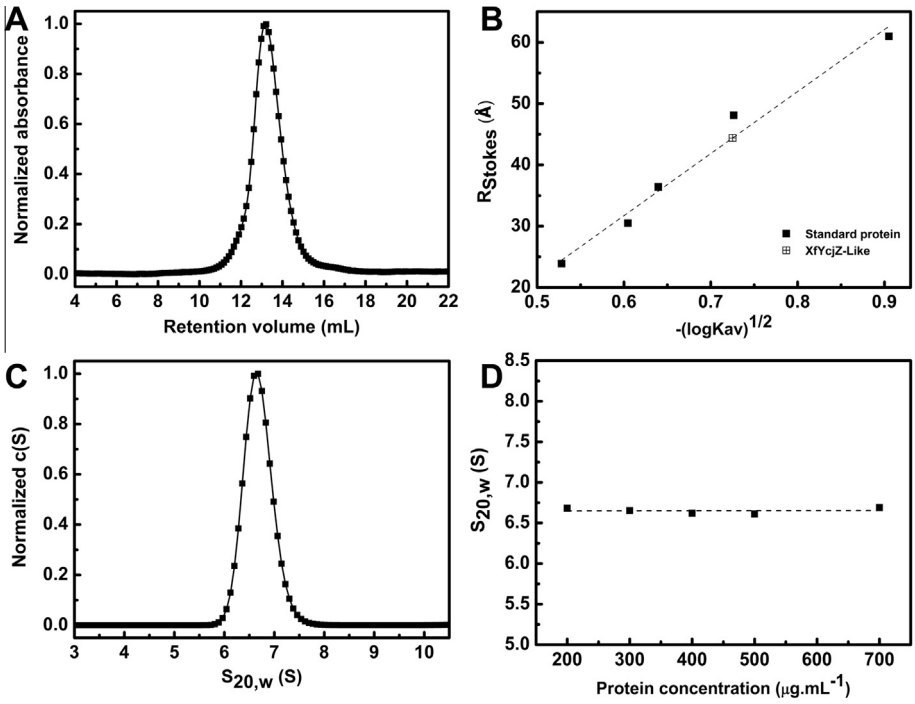

Fig. 3. Hydrodynamic properties of XfYcjZ-like. (A) Chromatogram of the analytical SEC experiments for recombinant, purified XfYcjZ-like protein. (B) The linear fitting of the Stokes radius (R_s) of the standard proteins (black square), carbonic anhydrase (Mw = 29 kDa, 23.9 Å), ovalbumin (Mw = 44 kDa, 30.5 Å), conalbumin (Mw = 75 kDa, 36.4 Å), aldolase (Mw = 158 kDa, 48.1 Å) and ferritin (Mw = 440 kDa, 61 Å) as a function of the values of $-(\log Kav)^{1/2}$ were used to estimate the R_s of the XfYcjZ-like as 44.4 ± 1 Å (open square). (C) Sedimentation velocity AUC experiments of XfYcjZ-like using a range of concentrations from 200 to 700 μg mL^{-1} in buffer (C). Panel C shows the c(S) distribution of XfYcjZ-like at 700 μg mL^{-1}. The sedimentation profiles show that one species predominated. (D) Dependence of XfYcjZ-like $s_{20,w}$ (S) as a function of protein concentration, which allowed us to obtain $s^0_{20,w}$ (S) of 6.65 ± 0.02. The hydrodynamic analyses indicated that XfYcjZ-like is a tetramer in solution.

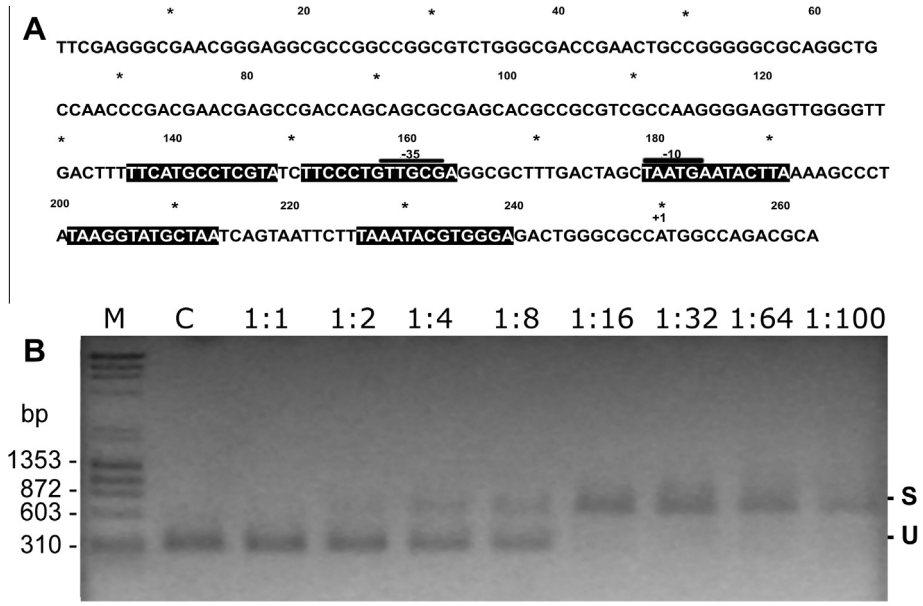

Fig. 4. XfYcjZ-like interacts with its own predicted promoter. (A) DNA sequence (262 bp) used in the EMSA analysis. The proposed -10 box and -35 box of the predicted *xfycjZ*-like promoter ($P_{xfycjZ\text{-like}}$) are indicated. +1 indicates the *xfycjZ*-like start codon. The LTTR predicted binding sites (T-N_{11}-A) are highlighted in black. (B) Interaction of XfYcjZ-like with its own putative $P_{xfycjZ\text{-like}}$. M, molecular weight marker; C, control reaction with the DNA fragment in the absence of protein; 1:1, 1:2, 1:4, 1:8, 1:12, 1:16, 1:32, 1:64 and 1:100 gradient of molar ratios of DNA:protein, considering the tetrameric form of XfYcjZ-like. The shifted bands (S) and unbound DNA fragment (U) are indicated on the right.

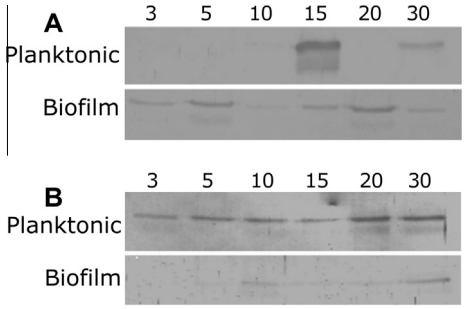

Fig. 5. Immunodetection of XfYcjZ-like during the *X. fastidiosa* planktonic and biofilm growth modes. (A) Detection of XfYcjZ-like during normal bacterial growth. (B) Detection of XfYcjZ-like after oxidative stress conditions were induced by a copper treatment. The numbers 3, 5, 10, 15, 20 and 30 correspond to the different days during biofilm growth. The associated planktonic cells were also collected. The total protein samples from each day were extracted, normalized using BCA quantification, and evaluated by Western blot using polyclonal antibodies against XfYcjZ-like.

is initiated; on the 15th day, the architecture of the biofilm begins to organize; and biofilm maturation occurs on the 20th day. Thus, XfYcjZ-like is involved in the development of the biofilm architecture and its maturation. These results are consistent with the involvement of the LTTRs in quorum sensing [34] and bacterial pathogenicity [35].

Interestingly, after a copper treatment, the detection of XfYcjZ-like in the planktonic cells was more pronounced (Fig. 5B), with it being detected on all of the days analyzed. Muranaka et al. [36] showed by microarray analysis that the ORF that encodes XfYcjZ-like was upregulated after oxidative stress was induced by copper treatment. Thus, our direct immunodetection findings confirmed that XfYcjZ-like is involved in the response to oxidative stress and can play a role in metal detoxification or metal homeostasis, as previously reported for *Enterococcus faecalis*, in which several LysR proteins were activated by copper [37]. Additionally, HbrL, which also belongs to the LTTR family of transcriptional regulators, in *Rhodobacter capsulatus* is responsive to iron [38].

The low response to copper during the different biofilm phases was intriguing (Fig. 5B). This result may have occurred because the *X. fastidiosa* biofilm is primarily composed of dead cells [39]. In this instance, a polysaccharide-rich gel layer is formed around the biofilm, which makes the biofilm less sensitive to environmental changes [40].

Conclusion

The LysR family participates in a myriad of cell functions, which range from cell division to bacterial pathogenicity. In this study, we attempted to understand the role of XfYcjZ-like during the developmental process of *X. fastidiosa* biofilm formation and during the response to copper. The formation of biofilms is considered the main pathogenicity mechanism of *X. fastidiosa*; therefore, understanding how this structure is formed can lead to the development of alternatives for controlling this phytopathogen. Our findings showed that XfYcjZ-like was upregulated by copper shock in planktonic cells and was involved in the organization of the architecture and maturation of biofilms and, consequently, in bacterial pathogenicity.

We hope to contribute to future studies focusing on the role that LTTRs, such as XfYcjZ-like, play in the modulation of gene expression, particularly during the phases in which the plant–bacteria interaction allows the bacteria (e.g., *X. fastidiosa*) to effectively colonize a susceptible plant, thus causing a specific disease.

Acknowledgments

This study was supported by Grants from the Fundação de Amparo à Pesquisa do Estado de São Paulo – Brazil (FAPESP, Process 2012/51580-4 and 2001/07533-7) and Coordenação de Aperfeiçoamento de Pessoal de Nível Superior (CAPES, Computational Biology Program). A.S.S. is the recipient of a Ph.D. fellowship from FAPESP (Process 2011/50268-4), CAS is the recipient of a Post-Doctoral fellowship, and A.P.S. is the recipient of a Research fellowship, both from the Conselho Nacional de

Desenvolvimento Científico e Tecnológico (CNPq). We gratefully acknowledge the Laboratório de Espectroscopia e Calorimetria (LEC), Laboratório Nacional de Biociências – LNBio (Campinas, Brazil), for their support of the CD and AUC studies.

References

[1] A.J. Simpson, F.C. Reinach, P. Arruda, F.A. Abreu, M. Acencio, R. Alvarenga, L.M. Alves, J.E. Araya, G.S. Baia, C.S. Baptista, M.H. Barros, E.D. Bonaccorsi, S. Bordin, J.M. Bove, M.R. Briones, M.R. Bueno, A.A. Camargo, L.E. Camargo, D.M. Carraro, H. Carrer, N.B. Colauto, C. Colombo, F.F. Costa, M.C. Costa, C.M. Costa-Neto, L.L. Coutinho, M. Cristofani, E. Dias-Neto, C. Docena, H. El-Dorry, A.P. Facincani, A.J. Ferreira, V.C. Ferreira, J.A. Ferro, J.S. Fraga, S.C. Franca, M.C. Franco, M. Frohme, L.R. Furlan, M. Garnier, G.H. Goldman, M.H. Goldman, S.L. Gomes, A. Gruber, P.L. Ho, J.D. Hoheisel, M.L. Junqueira, E.L. Kemper, J.P. Kitajima, J.E. Krieger, E.E. Kuramae, F. Laigret, M.R. Lambais, L.C. Leite, E.G. Lemos, M.V. Lemos, S.A. Lopes, C.R. Lopes, J.A. Machado, M.A. Machado, A.M. Madeira, H.M. Madeira, C.L. Marino, M.V. Marques, E.A. Martins, E.M. Martins, A.Y. Matsukuma, C.F. Menck, E.C. Miracca, C.Y. Miyaki, C.B. Monteriro-Vitorello, D.H. Moon, M.A. Nagai, A.L. Nascimento, L.E. Netto, A. Nhani Jr., F.G. Nobrega, L.R. Nunes, M.A. Oliveira, M.C. de Oliveira, R.C. de Oliveira, D.A. Palmieri, A. Paris, B.R. Peixoto, G.A. Pereira, H.A. Pereira Jr., J.B. Pesquero, R.B. Quaggio, P.G. Roberto, V. Rodrigues, M.R.A.J. de, V.E. de Rosa Jr., R.G. de Sa, R.V. Santelli, H.E. Sawasaki, A.C. da Silva, A.M. da Silva, F.R. da Silva, W.A. da Silva Jr., J.F. da Silveira, M.L. Silvestri, W.J. Siqueira, A.A. de Souza, A.P. de Souza, M.F. Terenzi, D. Truffi, S.M. Tsai, M.H. Tsuhako, H. Vallada, M.A. Van Sluys, S. Verjovski-Almeida, A.L. Vettore, M.A. Zago, M. Zatz, J. Meidanis, J.C. Setubal, The genome sequence of the plant pathogen *Xylella fastidiosa*. The *Xylella fastidiosa* consortium of the organization for nucleotide sequencing and analysis, Nature 406 (2000) 151–159.

[2] C.M. Rodrigues, A.A. de Souza, M.A. Takita, L.T. Kishi, M.A. Machado, RNA-Seq analysis of *Citrus reticulata* in the early stages of *Xylella fastidiosa* infection reveals auxin-related genes as a defense response, BMC Genomics 14 (2013) 676.

[3] M.W. LeChevallier, C.D. Cawthon, R.G. Lee, Inactivation of biofilm bacteria, Appl. Environ. Microbiol. 54 (1988) 2492–2499.

[4] J. Baker, S. Sitthisak, M. Sengupta, M. Johnson, R.K. Jayaswal, J.A. Morrissey, Copper stress induces a global stress response in *Staphylococcus aureus* and represses sae and agr expression and biofilm formation, Appl. Environ. Microbiol. (2010) 150–160.

[5] S. Chillappagari, A. Seubert, H. Trip, O.P. Kuipers, M.A. Marahiel, M. Miethke, Copper stress affects iron homeostasis by destabilizing iron–sulfur cluster formation in *Bacillus subtilis*, J. Bacteriol. 192 (2010) 2512–2524.

[6] P. Sornchuer, P. Namchaiw, J. Kerdwong, N. Charoenlap, S. Mongkolsuk, P. Vattanaviboon, Copper chloride induces antioxidant gene expression but reduces ability to mediate H_2O_2 toxicity in *Xanthomonas campestris*, Microbiology (Reading, England) 160 (2014) 458–466.

[7] E. Cabiscol, J. Tamarit, J. Ros, Oxidative stress in bacteria and protein damage by reactive oxygen species, Int. Microbiol. 3 (2000) 3–8.

[8] M.A. Schell, Molecular biology of the LysR family of transcriptional regulators, Annu. Rev. Microbiol. 47 (1993) 597–626.

[9] S.E. Maddocks, P.C. Oyston, Structure and function of the LysR-type transcriptional regulator (LTTR) family proteins, Microbiology (Reading, England) 154 (2008) 3609–3623.

[10] M.A. Toledo, D.R. Schneider, A.R. Azzoni, M.T. Favaro, A.C. Pelloso, C.A. Santos, A.M. Saraiva, A.P. Souza, Characterization of an oxidative stress response regulator, homologous to *Escherichia coli* OxyR, from the phytopathogen *Xylella fastidiosa*, Protein Expr. Purif. 75 (2011) 204–210.

[11] T. Shimada, K. Yamazaki, A. Ishihama, Novel regulator PgrR for switch control of peptidoglycan recycling in *Escherichia coli*, Genes Cells 18 (2013) 123–134.

[12] E.P. O'Grady, D.T. Nguyen, L. Weisskopf, L. Eberl, P.A. Sokol, The *Burkholderia cenocepacia* LysR-type transcriptional regulator ShvR influences expression of quorum-sensing, protease, type II secretion, and afc genes, J. Bacteriol. 193 (2011) 163–176.

[13] B.J. Habdas, J. Smart, J.B. Kaper, V. Sperandio, The LysR-type transcriptional regulator QseD alters type three secretion in enterohaemorrhagic *Escherichia coli* and motility in K-12 *Escherichia coli*, J. Bacteriol. 192 (2010) 3699–3712.

[14] H.R. Schlaman, B.J. Lugtenberg, R.J. Okker, The NodD protein does not bind to the promoters of inducible nodulation genes in extracts of bacteroids of *Rhizobium leguminosarum* biovar *viciae*, J. Bacteriol. 174 (1992) 6109–6116.

[15] K.A. Matthias, R.F. Rest, Control of pili and sialyltransferase expression in *Neisseria gonorrhoeae* is mediated by the transcriptional regulator CrgA, Mol. Microbiol. 91 (2014) 1120–1135.

[16] Z. Lu, M. Takeuchi, T. Sato, The LysR-type transcriptional regulator YofA controls cell division through the regulation of expression of ftsW in *Bacillus subtilis*, J. Bacteriol. 189 (2007) 5642–5651.

[17] M. Takao, H. Yen, T. Tobe, LeuO enhances butyrate-induced virulence expression through a positive regulatory loop in enterohaemorrhagic *Escherichia coli*, Mol. Microbiol. 93 (2014) 1302–1313.

[18] S. Lindquist, F. Lindberg, S. Normark, Binding of the *Citrobacter freundii* AmpR regulator to a single DNA site provides both autoregulation and activation of the inducible ampC beta-lactamase gene, J. Bacteriol. 171 (1989) 3746–3753.

[19] K. Vercammen, Q. Wei, D. Charlier, A. Dotsch, S. Haussler, S. Schulz, F. Salvi, G. Gadda, J. Spain, M. Levin Rybtke, T. Tolker-Nielsen, J. Dingemans, L. Ye, P. Cornelis, *Pseudomonas aeruginosa* LysR PA4203 regulator NmoR acts as a repressor of the PA4202 nmoA gene encoding a nitronate monooxygenase, J. Bacteriol. (2014).

[20] T. Kakuda, T. Hirota, T. Takeuchi, H. Hagiuda, S. Miyazaki, S. Takai, VirS, an OmpR/PhoB subfamily response regulator, is required for activation of vapA gene expression in *Rhodococcus equi*, BMC Microbiol. 14 (2014) 243.

[21] E. Stec, M. Witkowska-Zimny, M.M. Hryniewicz, P. Neumann, A.J. Wilkinson, A.M. Brzozowski, C.S. Verma, J. Zaim, S. Wysocki, G.D. Bujacz, Structural basis of the sulphate starvation response in *E. coli*: crystal structure and mutational analysis of the cofactor-binding domain of the Cbl transcriptional regulator, J. Mol. Biol. 364 (2006) 309–322.

[22] W.M. Zhang, J.J. Zhang, X. Jiang, H. Chao, N.Y. Zhou, Transcriptional activation of multiple operons involved in *para*-nitrophenol degradation by *Pseudomonas* sp. strain WBC-3, Appl. Environ. Microbiol. 81 (2015) 220–230.

[23] O. Porrua, M. Garcia-Jaramillo, E. Santero, F. Govantes, The LysR-type regulator AtzR binding site: DNA sequences involved in activation, repression and cyanuric acid-dependent repositioning, Mol. Microbiol. 66 (2007) 410–427.

[24] J. Sambrook, D.W. Russell, Molecular Cloning: A Laboratory Manual, third ed., Cold Spring Harbor Laboratory Press, Cold Spring Harbor, NY, 2001.

[25] A. Roy, A. Kucukural, Y. Zhang, I-TASSER: a unified platform for automated protein structure and function prediction, Nat. Protoc. 5 (2010) 725–738.

[26] P. Schuck, M.A. Perugini, N.R. Gonzales, G.J. Howlett, D. Schubert, Size-distribution analysis of proteins by analytical ultracentrifugation: strategies and application to model systems, Biophys. J. 82 (2002) 1096–1111.

[27] R. Caserta, M.A. Takita, M.L. Targon, L.K. Rosselli-Murai, A.P. de Souza, L. Peroni, D.R. Stach-Machado, A. Andrade, C.A. Labate, E.W. Kitajima, M.A. Machado, A.A. de Souza, Expression of *Xylella fastidiosa* fimbrial and afimbrial proteins during biofilm formation, Appl. Environ. Microbiol. 76 (2010) 4250–4259.

[28] E. Perez-Rueda, J. Collado-Vides, Common history at the origin of the position-function correlation in transcriptional regulators in archaea and bacteria, J. Mol. Evol. 53 (2001) 172–179.

[29] J.L. Taylor, R.S. De Silva, G. Kovacikova, W. Lin, R.K. Taylor, K. Skorupski, F.J. Kull, The crystal structure of AphB, a virulence gene activator from *Vibrio cholerae*, reveals residues that influence its response to oxygen and pH, Mol. Microbiol. 83 (2012) 457–470.

[30] Y. Zhang, J. Skolnick, Scoring function for automated assessment of protein structure template quality, Proteins 57 (2004) 702–710.

[31] G. Vadlamani, M.D. Thomas, T.R. Patel, L.J. Donald, T.M. Reeve, J. Stetefeld, K.G. Standing, D.J. Vocadlo, B.L. Mark, The beta-lactamase gene regulator AmpR is a tetramer that recognizes and binds the D-Ala-D-Ala Motif of its repressor UDP-MurNAc-pentapeptide, J. Biol. Chem. (2014).

[32] K. Goethals, M. Van Montagu, M. Holsters, Conserved motifs in a divergent nod box of *Azorhizobium caulinodans* ORS571 reveal a common structure in promoters regulated by LysR-type proteins, Proc. Natl. Acad. Sci. USA 89 (1992) 1646–1650.

[33] M.R. Parsek, R.W. Ye, P. Pun, A.M. Chakrabarty, Critical nucleotides in the interaction of a LysR-type regulator with its target promoter region. catBC promoter activation by CatR, J. Biol. Chem. 269 (1994) 11279–11284.

[34] A. Ilangovan, M. Fletcher, G. Rampioni, C. Pustelny, K. Rumbaugh, S. Heeb, M. Camara, A. Truman, S.R. Chhabra, J. Emsley, P. Williams, Structural basis for native agonist and synthetic inhibitor recognition by the *Pseudomonas aeruginosa* quorum sensing regulator PqsR (MvfR), PLoS Pathog. 9 (2013) e1003508.

[35] C. Tam, O. Demke, T. Hermanas, A. Mitchell, A.P. Hendrickx, O. Schneewind, YfbA, a *Yersinia pestis* regulator required for colonization and biofilm formation in the gut of cat fleas, J. Bacteriol. 196 (2014) 1165–1173.

[36] L.S. Muranaka, M.A. Takita, J.C. Olivato, L.T. Kishi, A.A. de Souza, Global expression profile of biofilm resistance to antimicrobial compounds in the plant-pathogenic bacterium *Xylella fastidiosa* reveals evidence of persister cells, J. Bacteriol. 194 (2012) 4561–4569.

[37] M. Latorre, J. Galloway-Pena, J.H. Roh, M. Budinich, A. Reyes-Jara, B.E. Murray, A. Maass, M. Gonzalez, *Enterococcus faecalis* reconfigures its transcriptional regulatory network activation at different copper levels, Metallomics 6 (2014) 572–581.

[38] S. Zappa, C.E. Bauer, The LysR-type transcription factor HbrL is a global regulator of iron homeostasis and porphyrin synthesis in *Rhodobacter capsulatus*, Mol. Microbiol. 90 (2013) 1277–1292.

[39] S. Chatterjee, R.P. Almeida, S. Lindow, Living in two worlds: the plant and insect lifestyles of *Xylella fastidiosa*, Annu. Rev. Phytopathol. 46 (2008) 243–271.

[40] P.A. Cobine, L.F. Cruz, F. Navarrete, D. Duncan, M. Tygart, L. De La Fuente, *Xylella fastidiosa* differentially accumulates mineral elements in biofilm and planktonic cells, PLoS One 8 (2013) e54936.